A Developmental Approach to Visually-Guided Reaching in Artificial Systems

Giorgio Metta and Giulio Sandini

Lira Lab
DIST - University of Genova
Italy

Jürgen Konczak

Department of Psychology
University of Düsseldorf
Germany

Contact person:
Giulio Sandini
University of Genova - Via Opera Pia, 13
16143 Genova - Italy
Tel: +39(10)3532779
Fax: +39(10)3532154
E-mail: giulio@dist.unige.it

Running title: Development in Artificial Systems

Preprint submitted to Neural Networks *7 June 1999*

A Developmental Approach to Visually-Guided Reaching in Artificial Systems ⋆

Abstract

The aim of the present paper is to propose that the adoption of a framework of biological development is suitable for the construction of artificial systems. We will argue that a developmental approach does provide unique insights on how to build highly complex and adaptable artificial systems. To illustrate our point, we will use as an example the acquisition of goal-directed reaching. In the initial part of the paper we will outline a) how mechanisms of biological development can be adapted to the artificial world, and b) how this artificial development differs from traditional engineering approaches to robotics. An experiment performed on an artificial system initially controlled by motor reflexes is presented, showing the acquisition of visuo-motor maps for ballistic control of reaching without explicit knowledge of the system's kinematic parameters.

Key words: Development, Learning, Motor control, Human infants, Robotics, Artificial systems.

⋆ The research described here is supported in part by a National Project of the Italian Ministry of Scientific and Technological Research (MURST), by Italian Space Agency (ASI) and in part by the EU-TMR project Virgo

1 Introduction

Research activity linking studies on artificial systems to "brain sciences" is certainly not new. Besides the studies on artificial neural networks, substantial efforts are devoted worldwide to building "physical models" of segments of biological systems with the aim of suggesting novel solutions to robotics or processing problems and to advance our understanding of human brain functions (Brooks, 1996; Sandini, 1997).

On the other hand the study of sensori-motor coordination in artificial systems has focused mainly on analyzing and implementing skill levels comparable to those of adult humans. For example, the control of robot heads and visually guided manipulation tasks were studied with reference to psychophysical performance data of adult humans and animals (Crowley, Bobet, & Mesrabi, 1992; Ballard, & Brown, 1992; Coombs & Brown, 1990; Aloimonos, Weiss, & Bandyopadhyay, 1988; Bajcsy & Tsikos, 1988; Bajcsy, 1985; Capurro, Panerai, Grosso, & Sandini, 1993; Capurro, Panerai, & Sandini, 1997; Capurro, Panerai, Grosso, & Sandini, 1996; Gandolfo, Sandini, & Tistarelli, 1991; Grosso, Metta, Oddera, & Sandini, 1996).

In spite of the recent advances in this area, the systems implemented are still far from achieving human-like performance levels and task flexibility. More importantly, even for successful implementations the integration of such skills as manipulation and gaze control proved to be more difficult than expected. In our view, this difficulty arises, at least in part, from the approach followed to construct complex systems: to make the problem more tractable, sensori-motor coordination is broken down into a set of sub-problems defined by a specific sensory modality (e.g. vision, audition, touch etc.) or specific motor skills (e.g. manipulation, gaze control, navigation).

A different solution is used in humans and many other vertebrates, where flexible and efficient levels of performance are achieved through the simultaneous development of sensory, motor and cognitive abilities. This process is not simply caused by the maturation of single components or by learning a progressively more sophisticated set of skills. Instead it is marked, particularly in the very early stages, by a sequence of changes of the neural circuitry, by a strategic exploitation of the environment with a limited set of motor skills that are present at each developmental stage, and finally, by the ability of biological systems to calibrate themselves in the presence of ongoing environmental and internal (e.g. anthropometric) changes.

In this view development is not a mere summation of discrete learning events. The degree of learning is determined by the learner's developmental state, which in turn is the result of complex interactions of maturational and en-

dogenous processes with the environment.

We have now a reasonable understanding of the developmental progression of reaching in infants. Yet, a mere description of a process of biological development does not shed any light to the issue of how physiological mechanisms of development are helpful for building complex artificial systems. A second step is necessary to bridge this gap. This step is to outline the control problems that have to be solved by human infants when trying to reach for objects in their immediate workspace. As we will see, the control problems for newborn humans and a robot may be expressed in a similar way in spite of the different "technologies" used for the actuators and sensing elements. For the sake of our argument at this point, let us divide the human organism into two distinct elements - the central nervous system (CNS) as the "controller", and the body as the "plant" (We realize that this is an undue simplification).

The first question to ask in the context of motor control is: what physiological or movement parameters does the system actually have to control to achieve its goal of reaching for a target in extrapersonal space? To answer this question, consider that each limb segment of the human arm is moved by a set of actuators with spring-like properties. In order to control the arm in a coordinated manner any controller needs to have at least reasonable approximations of inertia, viscosity and stiffness parameters.

That is, a first step for a control system must be the identification of the plant's parameters. A second step before goal-directed reaches are possible is the mapping of sensory maps onto available motor maps. That is, the system must be able to localize objects in extrapersonal space, and should have a knowledge where its limbs are positioned relative to the object. In a traditional learning paradigm, these two processes of calibration have to be completed before the system can begin to work on control (Kalveram, 1991; Kuperstein, 1988).

Today the view of a parallel development of calibration and control processes seems widely accepted by researchers working on neural modeling of adaptive eye-hand coordination (Jordan, 1996; Kawato, Furukawa, & Suzuki, 1987). Yet, most researchers model this process as a learning and not as a developmental operation (Jordan & Flash, 1994; Kuperstein, 1988). Implicit to such an approach of artificial eye-hand coordination is the premise that all behaviors of the system have to be learned. However, this assumption is not necessarily true for biological systems. One major difference between a biological and artificial system is that a biological system does not come as a "blank slate". In a wide variety of different species one can observe stereotyped inborn movement sequences that are clearly unlearned. Ethologists have argued for a long time that many behaviors, especially those of lower animals, cannot be explained on the basis of sensori-motor learning alone (Eibl-Eibesfeld,

1970; Gould, 1982). Newborn human infants already possess a repertoire of coordinated movements. For example, they can perform a series of complex multi-joint bilateral movements (i.e. kicking) and have available a set of so-called primitive reflexes. These primitive reflexes resemble a set of complex movement patterns that are triggered by a sensory stimulus.

Yet, these motor primitives may also serve a second function. They help to build up a relationship between vision and proprioception. For example, during pre-reaching the presence of the Asymmetric Tonic Neck Reflex (ATNR) plays a crucial role in allowing babies to see their hand and in increasing visual fixation of the hands (White, Castle, & Held, 1964; Bushnell, 1981) [1]. Thus, this multi-muscle synergy coupling arm and head movements provides an effective mean for linking visual and proprioceptive maps.

2 Developmental Engineering

Some of the peculiarities of human development outlined in the previous section are particularly relevant from the engineering perspective of building a complex adaptive system.

The first, and perhaps the major, observation relates to the fact that during the developmental process the infant is a self-contained, functional system with matched sensorial, motor and cognitive abilities. Motor reflexes and sensory-triggered motions are present at birth, exploiting the still limited sensory and motor abilities and allowing the infant to start some form of interaction with the environment and the acquisition of first sensori-motor experiences. During the initial months, some of the abilities are only temporarily present (for example, some of the early reflexes) and they disappear as soon as more mature skills develop. The control structure changes with age starting from an almost purely reflexive system at birth, passing through phases where basal muscular synergies are formed, towards a state where stable kinematic patterns are expressed - a sign that the redundant degrees of freedom of the neuromuscular system are then under voluntary control. From the engineering perspective this means a shift of emphasis from the "final product" to a "process-oriented" approach.

Another issue worth stressing is the role of the infant's own body in devel-

[1] The stimulus for the ATNR is the turning motion of the head, which subsequently will trigger a complex bilateral synergy. The infant's arm will be extended to the side the infant is looking, effectively bringing the hand into the field of view. The contralateral arm is flexed as part of crossed extensor reflex spanning both homologous limbs

opment. In biological systems, development is very much dependent on the ability of the system to interact with the external world. Many early sensorimotor experiences are stimulated by the newborn's own body motions which becomes an essential tool to establish a coupling between perception and action. On a neuronal level this organism-environment interaction is necessary to establish new connections, and to prune those that proved to be unfunctional (O'Leary, 1992). Self-generated motor commands elicit sensory feedback (like proprioceptive signals, motion in the visual field, tactile and acoustic stimuli) that not only give the newborn a motivation to repeat or to avoid a specific action, but also serve to adjust and refine the voluntary motor commands. The emergence of the distinction between what is and what is not controllable, is one of the first achievements of a system whose survival depends on its interaction with the outside world.

Based upon these observations we designed an experiment with a robot to demonstrate the utility of a developmental approach for the implementation of an adaptive system engaged in a visually guided reaching task.

2.1 Development of Visually Guided Reaching

If we consider an artificial system engaged in a reaching task, the number of motor degrees of freedom (*d.o.f.*) that have to be controlled in parallel can be as high as 10 or more. Learning how to control all these *d.o.f.* simultaneously, can be done, but requires most probably a very high number of trials to be performed, in order to reach the required sequence of motor commands.

In a classic control theory approach, some of the system's parameters required by the controller are estimated a priori while others are identified at run-time by means of ad-hoc calibration procedures (Yoshikawa, 1990). Subsequently, a general purpose or a customized control law is applied. After the calibration procedure the system becomes fully functional and changes of the internal parameters require re-calibration of the system (Papanikolopoulos & Khosla, 1993; Samson, Borgue, & Espiau, 1991). Following this approach the problem is simplified by an accurate design but it might require a lot of preliminary effort during the design process.

Other solutions suitable to learn how to control a complex systems have been proposed. Among them, the *feedback error learning* (Kawato et al., 1987) and the *reinforcement learning* (Sutton & Barto, 1998). Along the same line of research we designed an alternative solution based on direct motor primitives representing multi-joint synergies (i.e. for arm extension). In this case a single command may produce complex multi-joint coordinated movements without the voluntary control of each individual *d.o.f.* Examples of such multi-joint

synergies are the ATNR (see the previous section) and the grasping reflex which activates a coordinated grasping movement of the hand when the palm touches an object. In order for this approach to be feasible and effective, the crucial points are how to represent the motor primitives, the mechanisms of sensori-motor mapping, and their developmental rules.

2.1.1 Motor Primitives

Isolated skeletal muscles act like non-linear (visco-elastic) actuators whose length-tension properties are modulated by neuromuscular activation (Rack & Westbury, 1969). For the purpose of the present work, however, a simplified linear model of the muscles (Kandel, Schwartz, & Jessel, 1991) has been used to express the torque exerted by a muscle on each joint:

$$\tau = -a\kappa(q - q_0) \tag{1}$$

where q_0 is the actuator's resting position, a is the activation value which modulates the overall stiffness κ (i.e. the spring constant of the muscles).

Assuming this model, a possible procedure for coding motor primitives is the so-called force fields approach proposed by Mussa-Ivaldi and Bizzi ((Mussa-Ivaldi & Giszter, 1992; Gandolfo & Mussa-Ivaldi, 1993; Mussa-Ivaldi, Giszter, & Bizzi, 1993) recently extended to nonlinear visco-elastic actuators (Mussa-Ivaldi, 1997)). According to this theory the neuromuscular control of each joint can be described by means of a torque field expressed by:

$$\boldsymbol{\tau}(\mathbf{q}, a) \tag{2}$$

where $\mathbf{q}$ is the vector of generalized coordinate, a is the activation value and $\boldsymbol{\tau}$ is the generalized torque field.

In case of a multi-joint structure (such as a limb) the overall torque is expressed by:

$$\boldsymbol{\tau} = \sum_i \boldsymbol{\tau}_i(\mathbf{q}, a_i) \tag{3}$$

where a_i are the control parameters.

From the mechanical point of view, the system controlled by these actuators is passive. Consequently it has a stable Equilibrium Point (EP) in its space state $(\mathbf{q}, \dot{\mathbf{q}})$. The EP is a) the point where the torque field described by equation 3 is zero, b) the intersection of the actuators' angle-tension curves. It is worth noting that if we apply the torques described by equation 3 to the multi-joints

structure its state will eventually reach the EP (at equilibrium). Thus, the EP can be thought of as the point toward which the configuration is aiming at each instant of time.

In theory specification of the EP is enough to drive the system to a given configuration. On the other hand, experimental results in animals and humans (Mussa-Ivaldi et al., 1993) support a rather different view. In fact, it seems that movement is obtained by shifting the EP smoothly from the start to the end, rather than suddenly moving it to the target position. The sequence of EPs defines what is called a *virtual trajectory* (Hogan, 1985). It is worth noting that, due to the dynamic parameters of the arm, the actual arm's trajectory is different from the virtual trajectory (in other words it is like pulling a toy car with a rubber band: the trajectory in space of the pulling hand is different from the trajectory of the car because of the stretching of the rubber band).

The simplification (and in some sense the feasibility) of this schema comes from the experimental observation that any position of the EP in the arm's configuration space (and consequently its motion) can be obtained by a linear combination of a small number of motor primitives each represented as a torque field (the so-called *basis field* (Mussa-Ivaldi & Giszter, 1992; Mussa-Ivaldi et al., 1993)).

In our model, each motor primitive is a structure which activates a single or a group of actuators (see also figure 1). It is actually a synergy which combines (linearly) the effect of a set of actuators by activating them synchronously by means of only one control parameter (i.e. $a_i = C_j$). Primitives can be described by the following torque field:

$$\mathbf{T}_j(\mathbf{q}, C_j) = \sum_i I_{ji} \boldsymbol{\tau}_i(\mathbf{q}, C_j) \tag{4}$$

where $\boldsymbol{\tau}_i$ is the i^{th} actuator field, C_j the activation value and

$$I_{ij} = \begin{cases} 1 \text{ if the } j^{th} \text{ controller activates the } i^{th} \text{ actuator} \\ 0 \text{ otherwise} \end{cases} \tag{5}$$

$\mathbf{T}_j$ are exactly the basis fields as shown in figure 2. The total field $\mathbf{T}$ is expressed by the following:

$$\mathbf{T}(\mathbf{q}) = \sum_j \mathbf{T}_j(\mathbf{q}, C_j) = \sum_j \sum_i I_{ji} \boldsymbol{\tau}_i(\mathbf{q}, C_j) \tag{6}$$

We designed a priori the connections between actuators and primitives (through I_{ij}). Thus in our case the basis fields are fixed and embedded into the system.

The following table represents the I matrix:

Primitive (j)	Actuators (i)			
	1	2	3	4
1	1	0	1	0
2	0	1	0	1
3	1	0	0	1
4	0	1	1	0

where primitives are labeled with j and actuators with i as in equation 5.

Given this assumption, the task of the controller is to combine the basis fields by providing, for each point of the configuration space, a set of control parameters C_j. A schematic diagram of the controller is shown in figure 1 in the case of four basis fields and two joints.

A further simplification allowed by the force field approach comes from the fact that control parameters are not dependent on any particular frame of reference (Mussa-Ivaldi & Giszter, 1992). This is easily shown converting equation 6 into extrinsic coordinate. Let $\mathbf{x} = \Lambda(\mathbf{q})$ be the direct kinematics mapping of the arm and $\mathbf{J}_\Lambda = \frac{\partial \Lambda}{\partial \mathbf{q}}$ its Jacobian. For any configuration where $\mathbf{J}_\Lambda$ is not singular we can write:

$$\mathbf{J}_\Lambda^{-T} \boldsymbol{\tau} = \mathbf{F} \tag{7}$$

where $\mathbf{J}_\Lambda^{-T}$ is the transposed inverted Jacobian, $\boldsymbol{\tau}$ the torque vector and $\mathbf{F}$ the corresponding force vector in extrinsic coordinate. Substituting equation 7 into equation 6 and considering linear actuators (see equation 1), yields:

$$\mathbf{J}_\Lambda^{-T} \mathbf{T} = \sum_j C_j \mathbf{J}_\Lambda^{-T} \mathbf{T}_j \tag{8}$$

where $\mathbf{J}_\Lambda^{-T} \mathbf{T} = \mathbf{F}$ is the total force field and $\mathbf{J}_\Lambda^{-T} \mathbf{T}_j = \mathbf{F}_j$ are the basis fields in extrinsic coordinate. Substituting yields:

$$\mathbf{F} = \sum_j C_j \mathbf{F}_j \tag{9}$$

Equation 9 shows that the control coefficients C_j are invariant under coordinate transformation (for a discussion of the underlying conditions see (Mussa-Ivaldi & Giszter, 1992)).

A similar result applies for the redundant case (where $\mathbf{J}_\Lambda$ is not invertible) depending on the motor primitives considered (Gandolfo & Mussa-Ivaldi, 1993). It is correct, given these results, to freely exchange torque fields generated by actuators with force fields applied to the arm end-point because the two representations are indeed equivalent.

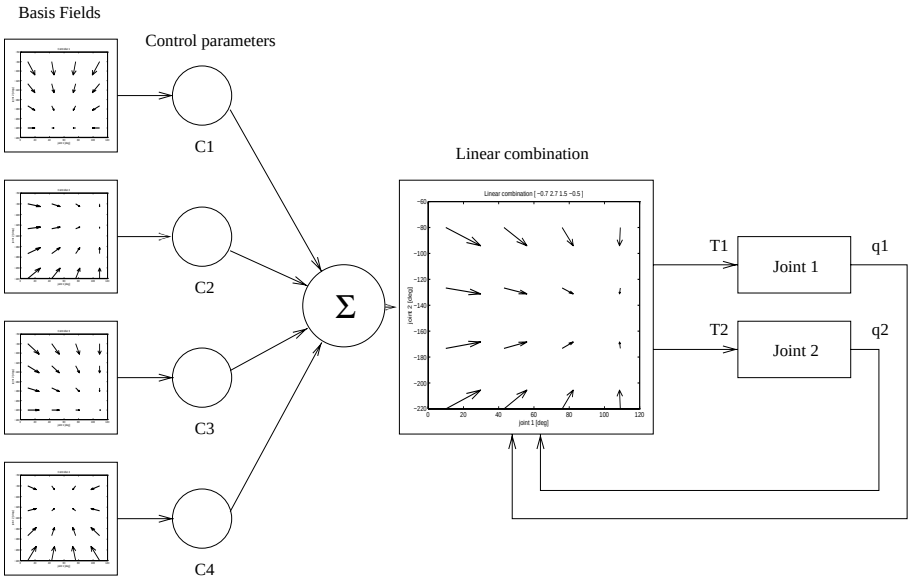

Fig. 1. Controller structure: motor primitives, represented by torque fields are combined (weighted by C_1, C_2, C_3 and C_4). The overall field "guides" the arm end-point toward its EP.

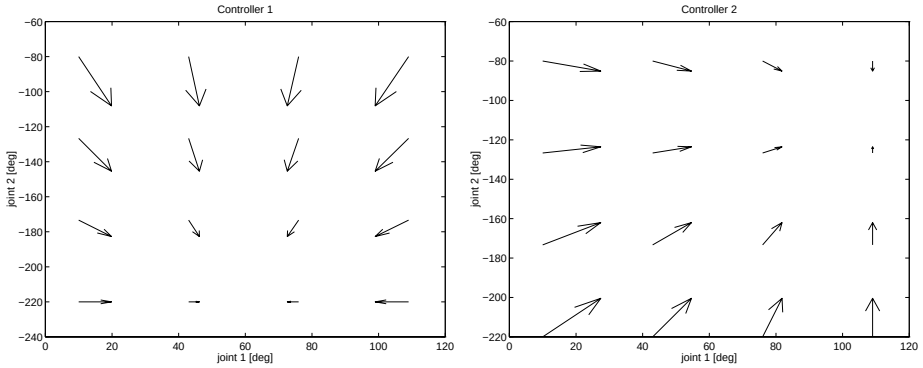

Fig. 2. Two of the four basis fields represented as torque fields in joints coordinates (see also figure 1 and 3). Ordinate and abscissa show joint position (joint 1 and 2) in degrees. Arrows point to the common EP of the two joints. Actual resting position of each actuator q_0 was preset by the experimenter.

From the developmental point of view, this approach is advantageous for two reasons: i) the kinematic parameters are embedded in the resulting force field (Hogan, 1985), and ii) each force field corresponds to the activation of a synergy of muscles and does not require the coordinated control of each degree of freedom. Furthermore the "innate" motor synergies can be easily represented through basis fields (or a combination of them). Figures 2 and 3 show two exemplar basis fields as used in our experiments. Figure 2 shows two torque fields

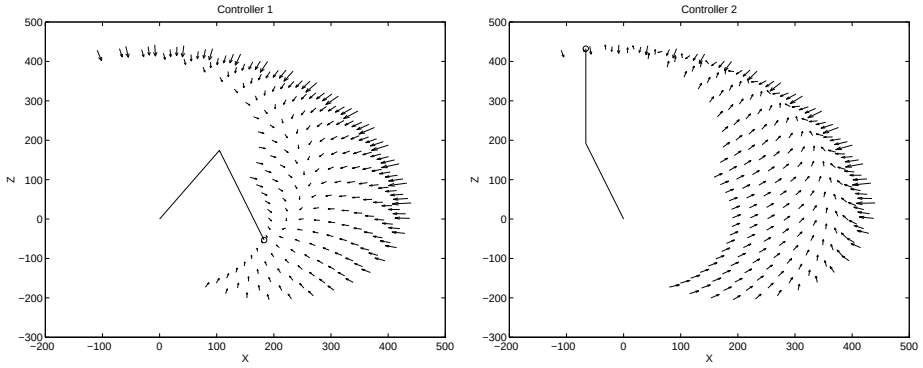

Fig. 3. Two of the four basis fields represented in cartesian coordinates (see also figure 2). Ordinate and abscissa represents the plane where the arm motion has been constrained.

Fig. 4. Equilibrium robot positions corresponding to the exemplar basis fields depicted in figure 2 and 3.

in joint coordinate while Figure 3 plots the corresponding two fields converted in cartesian coordinate. The pictures in Figure 4 shows the corresponding positions of our robot at equilibrium.

2.1.2 Motor-motor coordination

Let us now address the issue of how to drive the motor plant with positional information obtained by vision. In other words, we want to define a way of transforming the visually specified, spatial position of the target into the control parameters C_j. If this task were implemented on the basis of the cartesian position of the target in space, the kinematics of the eye-head system as well as of the arm, would have to be explicitly considered in order to select (or combine) the appropriate force fields. The solution we propose is based on the use of a direct mapping between the eye-head motor plant and the arm motor plant. One premise we make is that the position of the fixation point coincides (at least at some stage of the control process) with the object to be reached. In other words, the reaching of an object starts by looking at it. Under this assumption, the fixation point can be seen as the "end-effector" of the eye-head system and its position in space with respect to the shoulder is uniquely

determined by the motor commands controlling the position of the head with respect to the torso and that of the eyes with respect to the head. In other words, the position in space of the fixation point can be coded directly using motor commands i.e. any set of parameters used to control the gaze direction. Mapping these motor parameters into the arm's force field is what is required to coordinate visual information and motor control.

The system learns the transformation by collecting pairs of vector of the form "head control vector"-"arm control vector" while interacting with the environment. We call this approach *motor-motor coordination* (Gandolfo, Sandini, & Bizzi, 1996), because the coordinated action is obtained by mapping motor commands onto motor commands. It is also worth noting that the resulting map is, indeed, a representation of the end-effector command in egocentric coordinates and it is consequently in agreement with recent biological findings (Laquaniti & Caminiti, 1998).

3 The experiment

Based upon the choices presented in the previous sections an experiment was designed to show how reaching behaviour can be acquired by building a map from the head activation values to arm activation values.

In this experiment a four degrees of freedom set-up was used: two d.o.f. to control the gaze direction of the camera and two, controlling the position of the end-effector on a plane. The position of the head and arm resembles an anthropomorphic structure and their relative position is fixed but unknown to the system. The visual part is based on a color camera with a space-variant distribution of sensing element generating images with about 2,000 pixels in a log-polar format (Sandini & Tagliasco, 1980; Sandini, Gandolfo, Grosso, & Tistarelli, 1993; Capurro et al., 1997; Panerai & Sandini, 1998). The processing is distributed between a Pentium 200 computer and a Sun workstation controlling the arm using the RCCL software package (Lloyd, 1992). The two systems are linked through a TCP/IP ethernet connection.

The following constraints were imposed to obtain the real-time performance required. First, the visual localization of target and end-effector is based on a simple color segmentation algorithm. The target is identified by a green region and the end-effector by a red one (in both cases the position of the segmented region in the image plane is identified by the center of gravity). The second constraint is that only the arm motion is learned while the mapping between the position of the target in the image plane and the eye's motor command required to fixate the target is tuned beforehand. Lastly, the representative control parameters we choose in order to describe the head plant (gaze di-

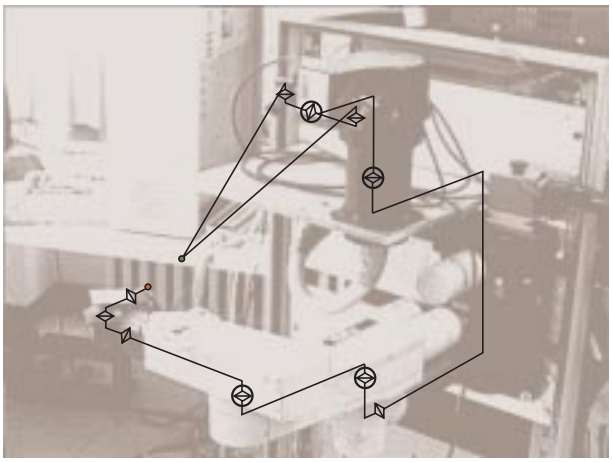

Fig. 5. The experimental setup. It consists of a ten degrees of freedom robot, links are indicated by continuous lines. The two links originating from the cameras are "virtual" and their intersection represent the fixation point (the end-effector of the head system). Joints are depicted as small quadrilaterals, their axis of rotation are along the corresponding links. The four joints utilized in our experiments are marked with a superimposed circle.

rection) were the joint angular positions. It is fair to say that there are at least two possible choices: 1) joint positions, 2) head activation values. Both solutions provide their own advantages and drawbacks. We choose to use joint positions in order to keep implementation as simple as possible. Integration of a more interesting gaze control strategy (such as those described in (Berthouze & Kuniyoshi, 1998; Capurro et al., 1997; Panerai & Sandini, 1998)) is currently under implementation.

These constraints do not affect, in our view, the main points of the approach proposed. However is it fair to say that removing some of these constraints (e.g. introducing a redundant manipulator) may likely introduce new problems, not accounted for at this point.

Given these considerations the map, in this particular experiment, can be represented by:

$$\mathbf{C} = f(\mathbf{q}) \tag{10}$$

where f is the unknown true function which must be approximated by learning, $\mathbf{q} \in \Re^2$ is the head joint angle's vector and $\mathbf{C} \in \Re^4$ is the arm activation vector.

The $(\mathbf{q}, \mathbf{C})$ pairs required to estimate the function f are measured whenever the system is fixating its own hand (and not when the gaze is fixating the target). The values of the activation vectors $\mathbf{C}$ are stored in a look-up table (the motor-motor coordination map) whose input space $\mathbf{q}$ is sampled with

uniform resolution (a vector **C** can be stored in each location or "cell"). If a cell has never been visited, but the function value for that input position is needed, the value stored in the nearest visited cell is used instead. Learning proceeds by updating the values of **C** each time the corresponding head joint vector is used to fixate the end-effector.

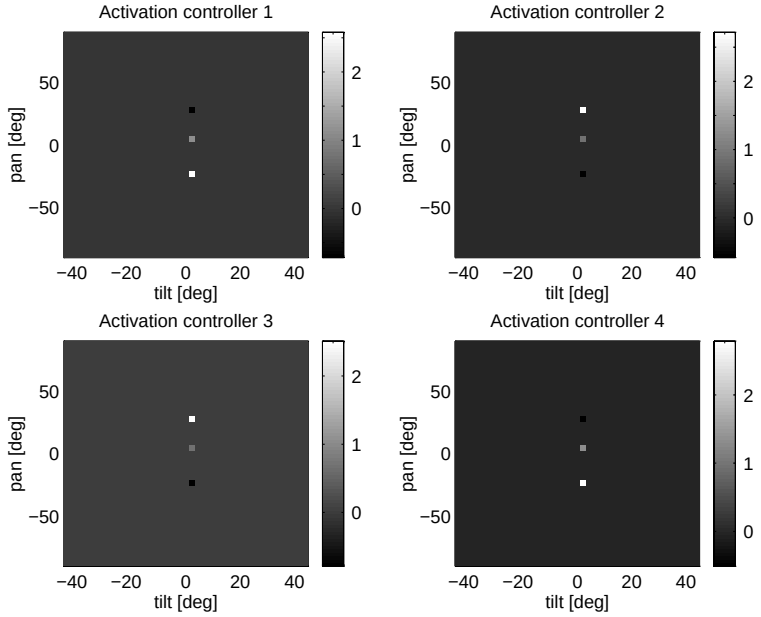

Fig. 6. Initial configuration of the head-arm mapping. Ordinate and abscissa are the head joint angles (in degrees). Grey levels represent the controllers activation value C_1, C_2, C_3 and C_4 as described in section 2.1.

3.1 Initialization of the Motor-Motor Map

The first problem to be solved is how to initialize the map in a meaningful way (or, in other words, what type of motor primitives should be used as the basis of the learning procedure). In natural systems this is obtained by reflexive mechanisms like the Asymmetric Tonic Neck Reflex which has the role of maintaining the arm within the field of view.

In our experiment, the robot utilizes a discrete approximation of the ATNR by initializing the head-arm map so that the arm is extended roughly in the direction the head is turned. As shown in Figure 6, each map stores three initial values of each of the four elements of the activation vector **C** corresponding to the three head position. The coordinate axes represent the head's tilt (abscissa) and pan (ordinate) angles.

Each map is virtually empty apart from the three "dots" representing the values **C** corresponding to three head positions (see Figure 6). The three activation vectors span uniformly the arm workspace and were computed so that

whenever they are used the arm end-point would move into the camera field of view. Consequently, even if the choice of just three positions is arbitrary, this initialization of the head-arm mapping is advantageous with respect to a random sampling of the workspace for two reasons. First the system is put in the conditions to be able to learn from visually measured errors (the arm is kept in the field of view) and second the intial values implicitely limit the explotation space to accessible and safe regions of the workspace.

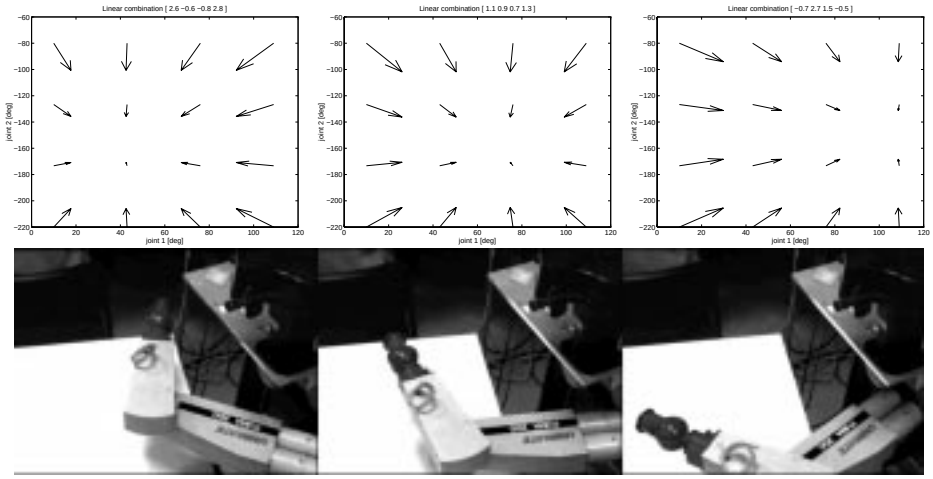

Fig. 7. Equilibrium arm position (lower row) and force fields corresponding to the three initial reflexes. Ordinate and abscissa (upper row) show joint position of respective joint. Arrows point to the common equilibrium position of the two joints. The three equilibrium positions have been preset by the experimenter.

The arm's postures corresponding to the initial values of $\mathbf{C}$ are shown in Figure 7. It is worth noting that initially the head can explore its entire workspace while only three positions of the arm are possible. The goal of the learning procedure is to fill the empty space of the maps.

3.2 Trajectory Generation

Both head and arm motion are controlled by torque values representing head and arm force fields. For the head, the instantaneous torque τ is obtained from the activation values C_i derived from the gaze error (see Figure 8). The gaze error is measured as the target position with respect to the image center expressed in image coordinates.

For example, if the target is located to the right of the fovea, the activation of the right muscle is increased by an amount proportional to the error, while the antagonist is inhibited (activation is decreased by the same amount). The same applies for the tilt axis controlling the up-down motion.

Because the arm has higher inertia and friction of the reduction gears, the

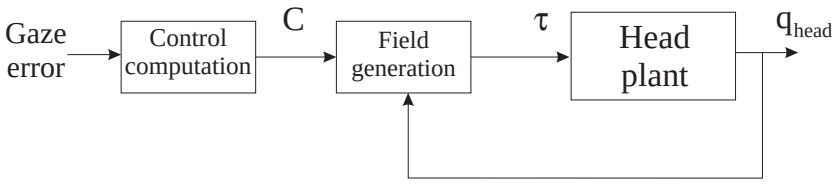

Fig. 8. Head control scheme. The position error is extracted from the image, converted and used directly to change the activation values of head actuators. The system in this case is using a closed loop approach as in the visual servoing paradigm.

extracted activation vectors $\mathbf{C}$ cannot be applied instantaneously. An instantaneous application of a torque step would bring the force outside the operational range of the motor. To avoid this situation, a mechanism transforming the activation values obtained by the map into smooth sequences is required. Such gradual rise in force is also observed in biological motion (Kandel et al., 1991). A possible biological mechanism for incremental rise in force levels is motor unit size, with smaller units discharging first during the contraction (Hennemann's size principle) (Hennemann & Mendell, 1981).

To achieve a smooth rise in torque, we applied a linear interpolation for a fixed number of steps between the initial and the final activation values:

$$\mathbf{C}_{t+1} = \mathbf{C}_t + \frac{\mathbf{C}_{final} - \mathbf{C}_{initial}}{n_{steps}} \tag{11}$$

here $\mathbf{C}_t$ is the activation vector at the t^{th} time step, $\mathbf{C}_{final}$ is the target activation vector, $\mathbf{C}_{initial}$ its value when the command was issued, and n_{steps} the number of steps.

This interpolation procedure is particularly effective in our case because, even if new activation values are issued at approximately 1Hz (due to the visual and learning processes), the arm controller (running at 50Hz) can easily generate the interpolated values.

At each time instant t, it is possible to determine an EP which is a function of $\mathbf{C}_t$ by imposing:

$$\mathbf{T} = \sum_j \mathbf{T}_j = \sum_j C_j \sum_i I_{ji} \boldsymbol{\tau}_i = \mathbf{0} \tag{12}$$

and solving for q.

The sequence of EPs defines the arm's virtual trajectory (see also section 3.4). However, it should be also considered that the sequence of $\mathbf{C}$ through time determines the shape of the trajectory. $\mathbf{C}_t$ can be considered as a set of parameters which are in principle learnable. In fact, they could be tuned in order to straighten the trajectories or to reduce overshoots.

Consider the usual Lagrange equation for a planar manipulator:

$$\mathbf{T} = A(\mathbf{q})\ddot{\mathbf{q}} + B(\mathbf{q}, \dot{\mathbf{q}}) \tag{13}$$

where $\mathbf{T}$ is the generalized torque applied to the arm. Substituting the expression for $\mathbf{T}$, generated by the set of elastic actuators and controllers as previously defined, yields:

$$\sum_j C_j \sum_i I_{ji} \boldsymbol{\tau}_i = A(\mathbf{q})\ddot{\mathbf{q}} + B(\mathbf{q}, \dot{\mathbf{q}}) \tag{14}$$

Two considerations stem from the previous equation: i) the real trajectory of the arm is determined by the shape and evolution in time of the torque field (left hand side of equation); ii) as already pointed out, the shape of the torque field is controlled by $\mathbf{C}_t$. If the system were able to tune $\mathbf{C}_t$ beside the simple linear interpolation, it could also change the resulting arm trajectory precisely. Although this could be a sensible strategy (for example to learn how to get a straight trajectory instead of a curved one) it was beyond the available computational power of our system.

The overall control scheme is shown in figure 9. The first stage of the processing is implemented in the map containing the arm activation vector. These values are interpolated and the output from the trajectory generator is sent to the actuators simulator (identified by the block "Field") which generates the torque commands.

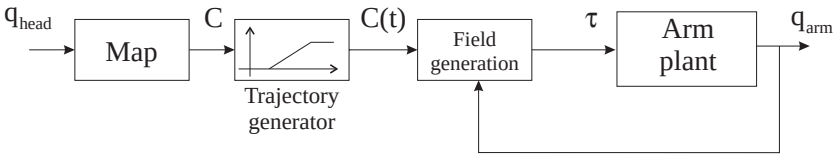

Fig. 9. The overall arm's control scheme. The position of the head (q_{head}) addresses the map which outputs the activation vector for the arm. This stage is followed by a trajectory generation which interpolates linearly between activation vectors. The resulting force field is then computed and used to generate the torques which drive the arm motors.

The learning algorithm can be formally described as follows:

Repeat forever.

(1) A proper stimulus appears in the field of view.

(2) By fixating the visual target the robot also initiates arm motion by computing the arm activation vector $\mathbf{C}$ in the following way:

$$\hat{f}_i(\mathbf{q}) + \mathbf{n} \tag{15}$$

The term $\mathbf{n}$ describes a zero-mean uniform noise component introduced to simulate errors in the arm control. $\hat{f}_i$ is the estimate of f at the i^{th} iteration.

(3) The vector $\mathbf{C}$ is used by the arm controller which computes the actual torques to drive the motors and consequently the arm moves toward the new EP.

(4) At this point the arm is as close as possible to the target (initially it is not very close but certainly it is in the field of view) so that the system can re-direct the gaze to its own hand.

(5) As a result of the previous step a new pair $(\mathbf{q}, \mathbf{C})$ is available which is used to update the map by computing the value $\hat{f}_{i+1}(\mathbf{q})$ in the following way:

$$\hat{f}_{i+1}(\mathbf{q}) = \hat{f}_i(\mathbf{q})\frac{n_v - 1}{n_v} + \frac{\mathbf{C}}{n_v} \tag{16}$$

where n_v is the number of visits of the cell corresponding to $\mathbf{q}$.

(6) The arm then returns to a fixed resting position (near the chest).

It is important to note that if the procedure were noise-free the motion of the arm toward the target (end of step 3) would always bring the end-effector in the same final position and the system would not be able to learn (in fact it would always update the same cell of the map with the same vector $\mathbf{C}$). In human development, the system is not noise free at birth. For example, nerve growth is not completed giving rise to slowed nerve conduction that is prone to interference, which ultimately may lead to poor sensory data (i.e. low visual acuity) and noisy motor output (Kinney, Brody, Kloman, & Gilles, 1988; Konczak, Borutta, Topka, & Dichgans, 1995; Konczak, Borutta, & Dichgans, 1997; Konczak & Dichgans, 1997). In our experimental condition errors were introduced "naturally" by the friction of the arm reduction gears and "arti-

ficially" by introducing a noise term in the motor-motor transformation (see step 2). During learning and subsequent retention trials friction of the arm could not be altered. However, the artificial noise was removed, whenever we tested the accuracy of reaching movements.

A map obtained after a training period of about 5 minutes and consisting of approximately 100 trials is shown in Figure 10.

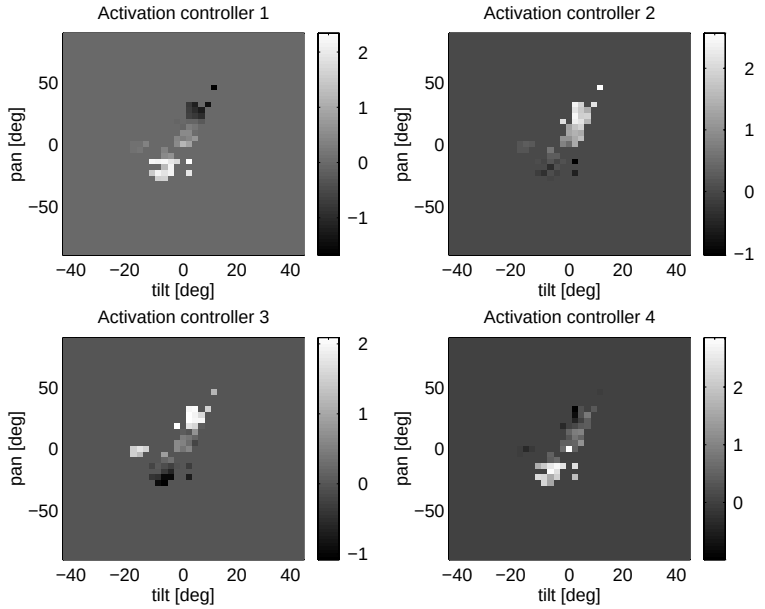

Fig. 10. Head-arm mapping after training. Ordinate and abscissa are the head joint angles (in degrees). Grey levels represent activation value C_1, C_2, C_3 and C_4 of each controller (see section 2.1).

A key point of the overall process, as it has been already pointed out, is the fact that the body plays both the role of the actor (by exploring the environment) and the role of the environment (by using the eye's fixation point as the target of the reaching process). This allows the overall system and the learning process to be self-contained and adaptive to kinematic and dynamic changes of the internal parameters (such as body segments length and weight) and moreover, the process is intrinsically egocentric. The motor-motor mapping, at least initially, does not necessarily bring the end-effector near to the fixation point (in fact it will bring the arm as close as possible to the target on the basis of what has been learned so far). However, instead of correcting the error by moving the arm, the direction of gaze is redirected to the end-effector and the arm motor command previously issued is associated to the new eye position. In other words, the role of the visual target appearing in the environment has the only function of initiating the arm motion while the learning process is based on the act of looking at the end-effector. As the learning process proceed, the initial arm motion gets closer and closer to the visual target and, eventually, the corrective gaze shift will not be necessary

unless kinematic changes occur.

3.4 Experimental results

Two different experiments were performed to illustrate the performance of the proposed approach. The first describes the learning of ballistic reaching movements toward static visual targets, the second presents the results of smooth coordinated eye-hand movements toward moving targets emerging from the learned ballistic behavior.

In order to test the performance of the system at different learning stages, the position in the arm's workspace of three targets was calibrated beforehand by manually positioning the end-effector at target center and storing the corresponding joint angle values measured by the encoders. Each target consisted of a piece of cardboard about 5×5cm in size.

During the training phase the target of the reaching task was manually moved by the experimenter over the arm's workspace while the reaching behavior was continuously activated. From time to time training was suspended and the performance evaluated.

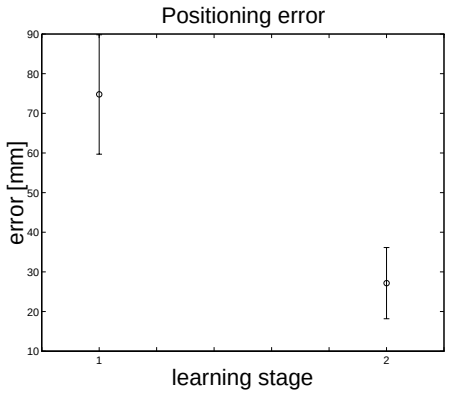

Fig. 11. Endpoint positioning error before and after learning. The error expresses the Euclidean distance between the end effector and the target at the end of reach. 134 movements were executed during the learning phase. The maximal achievable precision of the arm was 30mm.

During the evaluation phase the three targets in the calibrated positions were activated one at a time and the trajectory of the arm stored. The reaching error was measured by computing the Euclidean distance between the pre-calibrated target positions and the position of end-effector at the end of the reaching movement. At least 30 trials (10 for each target) were executed and the average error and standard deviation were computed. During this evaluation phase the map update was stopped and the noise term removed (see equation (15)).

The error before and after the execution of 134 learning movements is shown in Figure 11.

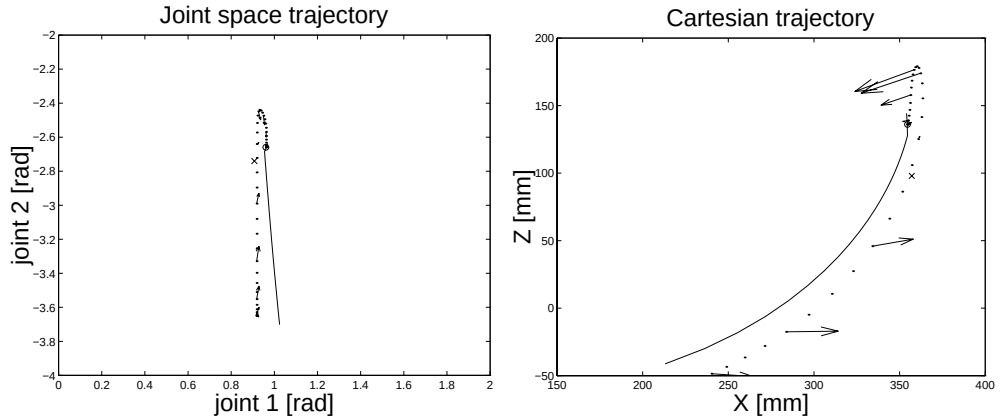

Fig. 12. Typical arm trajectory in joint (left) and Cartesian (right) coordinates. Dotted lines plot the real arm trajectories, continuous lines plot virtual trajectories. $\circ$ is the final end-point position and $\times$ is the actual position of the target. The vectors plotted every 5 data points are torques in joint space (as generated by the motors) and forces in the cartesian space. Left: joint 1 is the shoulder position while joint 2 refers to the elbow. Right: the XZ plane is the horizontal plane where the robot motion has been constrained.

It is important to note that trajectories are not learned by the system. They are just a consequence of the applied control strategy as described in section 3.2. A typical arm trajectory (after training) in joint and cartesian coordinates is shown in Figure 12. Both plots show the virtual (continuous line) and the actual (dotted line) trajectory of the arm and, "$\times$" represents the actual position of target while "$\circ$" shows the final position of the end-effector. Arrows represent torque in joint coordinates and force in cartesian coordinates. It is quite clear in both graphs the presence of an overshooting in the real trajectories. This is the effect of not knowing the dynamic parameters of the arm and particularly of the arm's inertia. As a consequence the torque applied in the initial part of the movement brings the end-effector beyond the target. The "force field approach", however, corrects this overshoot by applying a force in the opposite direction and partially compensates this lack of dynamic information. In our current schema there is no possibility to "learn" how to avoid this overshoot because this would require the tuning of other parameters such as the stiffness or the presence of compensating modules which explicitly take into account dynamics (Ghez, Gordon, Ghilardi, & Sainburg, 1996).

Similar considerations can be drawn by observing the plots in Figure 13. In this case reaching movements toward three different targets (at the end of the training phase) are shown in Cartesian coordinates. Trajectory toward target 1 shows the same overshoot described for Figure 12. The opposite happens when the most distant target 3 is reached. In this case the end-effector undershoots the target. Also in this case the remaining error can be attributed (in

part to intrinsic errors of the learning process) but also to the accumulation of errors deriving from friction (which is not only unknown but also partly unpredictable). Trajectory toward target 2 shows a back-and-forth motion with the final position reached after a couple of adjustments. This behavior is caused by the fact that the system is continuously operating and, consequently, whenever the end-effector partially covers the target, the head shifts the fixation point over the center of gravity of the remaining visible part. This change of fixation generates a new "force field" and, consequently a new trajectory. Eventually the visible part of the target does not change (the center of gravity of the target does not move any more) and the arm reaches its final position.

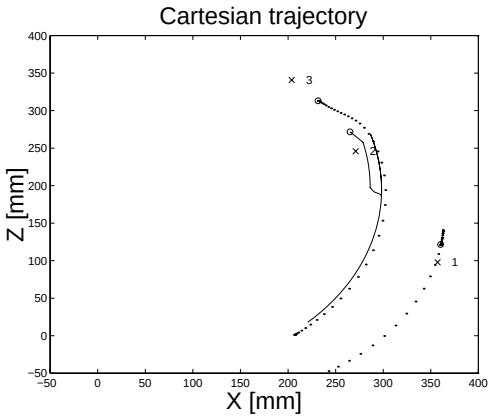

Fig. 13. Trajectories generated by reaching for three different targets. As in the previous figures, dotted lines represent the actual end-point trajectories in Cartesian coordinates. The solid line is relative to the reaching trial directed toward target 2. "∘" represent the final end-point positions and "×" the target positions.

At the end of the training phase the system was also tested in a different experimental condition, namely, during reaching of a smoothly moving target. In this case both the head and the arm are continuously moving to track the target. It is worth noting, that this condition was totally new for the system which, during the training phase, was programmed to move to a fixed starting position (with the arm flexed toward the "body") after each reaching motion.

The left panel of Figure 14 demonstrates the performance of the system before training. The arm motion was composed of two movement units each corresponding to one of the three initial force fields. The movement was dysmetric. The endpoint missed the target by nearly 10 cm. The right panel shows an exemplar endpoint trajectory after training.

Note that the endpoint path is smoother, corresponding to a better tracking performance. Endpoint error at movement termination was drastically reduced.

The remaining small oscillations are due mainly to the discrete nature of the look-up table approximating the map and to some amount to the scheme

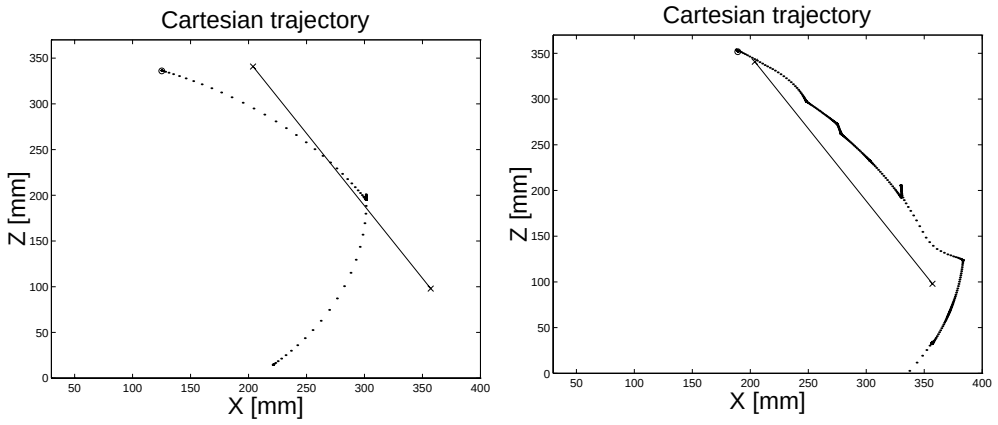

Fig. 14. Tracking a moving target. Abscissa and ordinate are the X and Z position represented respect to the arm base frame. The target moves in both experiments from the lower-right to the upper-left position at constant velocity along a straight path (solid line). The dotted line represents the end-point trajectory. The left plot has been obtained using the map before training, the right one refers to the map after training.

applied to control the head movements. Beside this defect the enhancement of the positioning abilities is very noticeable.

4 Conclusion

In this paper, a framework for the implementation of adaptable sensori-motor strategies for visually guided reaching was presented. The implemented framework was inspired by studies on human development, and we attempted to achieve visuo-motor coordination by adopting biologically plausible control structures.

We demonstrated the development of visually-guided reaching from an initial state characterized by a set of reflexive behaviors. Subsequently, visuo-motor skills are acquired by refining the mapping between sensory information and motor commands. During this developmental progression there is no distinction between plant's calibration and control. In addition, the kinematic and dynamic parameters are not explicitly identified as in classical control theory approaches. This developmental process may be viewed as adaptive change towards competence (Keogh & Sugden, 1985). Here, adaptive change is not the same as learning. In distinguishing between learning and development, we regard learning as a function of development rather than development being the overall summation of a series of learnings (Piaget & Inhelder, 1969). This view implies that learning is shaped by the learner's developmental state. In practice, this means that the system incrementally adapts its learning goals to the evolving developmental state. Engineering such a process means being able

to define a sequence of events that cause the system to become incrementally more skilled. One way of looking at it is to model a developmental stage as a set of control variables (in our case motor but, in general, also sensory and cognitive) and to model the process of development as a progressive, adaptive selection of the learning parameters.

Consider the developmental state of an human infant at birth. That state is characterized by an incomplete visuo-motor map, by imprecise knowledge of the plant, by the availability of basal intra- and interlimb synergies and a set of primitive reflexes. This setup allows the infant to explore the environment even at that early age. The exact mechanisms of this ontogenetic process in the first weeks of life is still not clear. However, visuo-motor coordination is likely based on at least two motor maps: a spinal and a cortical one. We know today that most cortico-spinal projections are not differentiated at birth (O'Leary, 1992) and that spinal reflex circuits provide the system with the reflexes and basal synergies necessary to initiate simple interactions with the environment.

As maturation progresses, cortical control loop become operational, building a map based on existing reflexes and basal synergies. In this sense, there seems to be no need to assume a cortical suppression mechanism inhibiting spinal reflexes (Gesell, 1946; McGraw, 1946). Instead, the development of visuo-motor coordination looks more like a process during which the system learns how to "drive" the spinal motor primitives. The autonomy of the spinal motor system becomes evident after the disruption of cortical input. Spinal synergies are preserved and still functional (for a review: (Grillner, 1981)).

With our robot setup we attempted to follow a similar line of developmental events. We equipped our robot with a set of basal synergies represented by the basis fields and embedded in the system a set of initial visuo-motor reflexes simulating the Asymmetric Tonic Neck Reflex required to maintain the hand in the field of view. The biological parallelism was stressed also at the level of the actuators by simulating the elastic properties of the muscles and exploiting those properties by means of motor primitives based on force fields. Visual processing, although rather simple, was performed on images acquired by an anthropomorphic sensor simulating the space-variant distribution of photoreceptors in the human retina.

The implemented artificial system only simulates biological development in a rather crude fashion. Yet, it possesses a set of features that we think are promising for designing autonomous robots that can act flexibly in a visually specified environment. These features are:

- the system is complete in the sense that specific sensory and motor components develop simultaneously.
- the sight of the hand drives the learning of the motor-motor map. In this

respect, robot's body generates enough information to learn a map which guides the reaching for an external object (target). We are not saying that eye-hand coordination in humans is implemented through a direct motor to motor mapping. However, this remains a researchable question.

- the basal motor repertoire becomes part of the growing motor-motor map without requiring the explicit inhibition of "innate" motor reflexes. This is not to say that at some later developmental state inhibitory mechanisms will not be employed.

In summary, during learning a defined relationship between various sensory and motor subsystems constrains the kind of tasks that can be learned. Development takes place on a larger scale. It is not a series of discrete learning experiences, but is characterized as a process where the interrelationships between subsystems are not yet rigidly defined. Thus, the developing systems are therefore adaptable to a potentially larger range of tasks.

5 List of symbols

Symbol	Units	Description
$\mathbf{q}$	rad	Generalized coordinate vector (all joints are revolute)
q_0	rad	Resting point (in a spring-like equation)
$\vec{\tau}$	Nm	Torque field generated by an actuator
κ	$Kg \cdot m^2/s^2$	Stiffness coefficient
a	None	Activation coefficient (for the actuators)
C	None	Activation coefficient (for the controllers)
I	None	Connection matrix for the controller structure
$\mathbf{T}$	Nm	Torque field generated by a controller
$\mathbf{x}$	m	End-point position
Λ	None	Direct kinematics
$\mathbf{J}_\Lambda$	None	Manipulator Jacobian
$\mathbf{F}$	N	Force field for a controller
f	None	Motor-motor map
$\hat{f}$	None	Approximation of the motor-motor map
$\mathbf{n}$	None	Zero-mean, uniform distributed noise

References

Aloimonos, J., Weiss, I., & Bandyopadhyay, A. (1988). Active vision. *International Journal of Computer Vision*, *1*(4), 333–356.

Bajcsy, R., & Tsikos, C. (1988). Perception via manipulation. In *Proc. of the int. symp. & exposition on robots* (pp. 237–244). Sydney, Australia.

Bajcsy, R. K. (1985). Active perception vs. passive perception. In *Proc. third ieee workshop on computer vision: Representation and control* (pp. 13–16). Bellaire (MI).

Ballard, D., & Brown, C. (1992). Principles of animate vision. *Computer Vision Graphics and Image Processing*, *56*(1), 3–21.

Berthouze, L., & Kuniyoshi, Y. (1998). Emergence and categorization of coordinated visual behavior through embodied interaction. *Machine Learning*, *31*, 187-200.

Brooks, R. (1996). Behavior-based humanoid robotics. In *Proc. ieee/rsj iros'96* (Vol. 1, p. 1-8).

Bushnell, E. (1981). The ontogeny of intermodal relations: vision and touch in infancy. In R. Walk & H. Pick (Eds.), *Intersensory perception and sensory integration* (p. 5-37). New York: Plenum Press.

Capurro, C., Panerai, F., Grosso, E., & Sandini, G. (1993). A binocular active vision system using space variant sensors: Exploiting autonomous behaviors for space application. In *Int. conf. on digital signal processing.* Nicosia, Cyprus.

Capurro, C., Panerai, F., Grosso, E., & Sandini, G. (1996). Visuo-motor coordination for advanced robotics. In *6th isir international symposium on industrial robotic.* Milan, Italy.

Capurro, C., Panerai, F., & Sandini, G. (1997). Dynamic vergence using log-polar images. *International Journal of Computer Vision*, *24*(1), 79–94.

Coombs, D., & Brown, C. (1990). Intelligent gaze control in binocular vision. In *Proc. of the fifth IEEE international symposium on intelligent control.* Philadelphia, PA.

Crowley, J., Bobet, P., & Mesrabi, M. (1992). Gaze control with a binocular camera head. In *Proc. eccv92 - european conference of computer vision* (Vol. LNCS-588). Santa Margherita Ligure, Italy: Springer-Verlag.

Eibl-Eibesfeld, I. (1970). *Ethology: the biology of behavior (e.klinghammer trans.).* New York: Holt, Rinehart and Winston.

Gandolfo, F., & Mussa-Ivaldi, F. (1993). Vector summation of end-point impedance in kinematically redundant manipulators. In *Proc. of ieee/rjs international conference of intelligent robots and systems* (p. 1627-1634). Yokohama, Japan.

Gandolfo, F., Sandini, G., & Bizzi, E. (1996). A field-based approach to visuo-motor coordination. In *Proc. workshop on sensorimotor coordination: amphibians, models, and comparative studies.* Sedona, Arizona USA.

Gandolfo, F., Sandini, G., & Tistarelli, M. (1991). Towards vision guided

manipulation. In *Proc. intl. conference on advanced robotics '91.* Pisa, Italy.

Gesell, A. (1946). The ontogenesis of infant behavior. In L. Carmichael (Ed.), *Manual of child psychology* (p. 295-331). New York: Wiley.

Ghez, C., Gordon, J., Ghilardi, M., & Sainburg, R. (1996). Contribution of vision and proprioception to accuracy in limb movements. In M. S. Gazzaniga (Ed.), *The cognitive neuroscoences.* Cambridge: MIT-Press.

Gould, J. (1982). *Ethology: the mechanism and evolution of behavior.* New York: Norton.

Grillner, S. (1981). Control of locomotion in bipeds, tetrapods, and fish. In V. Brooks (Ed.), *Handbook of physiology* (Vol. Section 1: The Nervous System, p. 1179-1236). Bethesda: American Physiological Society.

Grosso, E., Metta, G., Oddera, A., & Sandini, G. (1996). Robust visual servoing in 3d reaching tasks. *IEEE Trans. Robotics and Automation*, *12*(8), 732–742.

Hennemann, E., & Mendell, L. (1981). In V. Brooks (Ed.), *Handbook of physiology* (Vol. Sect. 1 Vol. 2 Part. 1, p. 423-507). Washington, D.C: American Physiological Society.

Hogan, N. (1985). The mechanics of multi-joint posture and movement control. *Biological Cybernetics*, *52*, 313-331.

Jordan, M. (1996). Computational motor control. In M. S. Gazzaniga (Ed.), *The cognitive neuroscoences.* Cambridge: MIT-Press.

Jordan, M., & Flash, T. (1994). A model of the learning of arm trajectories from spatial deviations. *Journal of Cognitive Neuroscience*, *4*(6), 359-376.

Kalveram, K. (1991). Controlling the dynamics of a two-joined arm by central patterning and reflex-like processing. a two stage hybrid model. *Biological Cybernetics*, *65*, 65-71.

Kandel, E., Schwartz, J., & Jessel, T. (1991). *Principles of neuroscience.* Elsevier.

Kawato, M., Furukawa, K., & Suzuki, R. (1987). A hierarchical neural network model for control and learning of voluntary movement. *Biological Cybernetics*, *57*, 169-185.

Keogh, J., & Sugden, D. (1985). *Movement skill development.* New York: Macmillan.

Kinney, H., Brody, B., Kloman, A., & Gilles, F. (1988). Sequence of central nervous system myelination in human infancy. ii.patterns of myelination in autopsied infants. *Journal of Neuropathology and Experimental Neurology*, *47*(3), 217-234.

Konczak, J., Borutta, M., & Dichgans, J. (1997). Development of goal-directed reaching in infants: Ii. learning to produce task-adequate patterns of joint torque. *Experimental Brain Research*, *113*, 465-474.

Konczak, J., Borutta, M., Topka, H., & Dichgans, J. (1995). Development of goal-directed reaching in infants: Hand trajectory formation and joint force control. *Experimental Brain Research*, *106*, 156-168.

Konczak, J., & Dichgans, J. (1997). Goal-directed reaching: development toward stereotypic arm kinematics in the first three years of life. *Experimental Brain Research*, *117*, 346-354.

Kuperstein, M. (1988). Neural model of adaptive hand-eye coordination for single postures. *Science*, *239*, 1308-1311.

Laquaniti, F., & Caminiti, R. (1998). Visuo-motor transformations for arm reaching. *European Journal of Neuroscience*, *10*, 195-203.

Lloyd, J. (1992). *Multi-rccl reference manual (release 4.2).* McGill University, Montreal.

McGraw, M. (1946). Maturation of behavior. In L. Carmichael (Ed.), *Manual of child psychology* (p. 332-369). New York: Wiley.

Mussa-Ivaldi, F. (1997). Nonlinear force fields: A distributed system of control primitives for representing and learning movements. In *Proceedings of cira'97.* Monterey, California, USA.

Mussa-Ivaldi, F., & Giszter, S. (1992). Vector field approximation: a computational paradigm for motor control and learning. *Biological Cybernetics*, *67*, 491-500.

Mussa-Ivaldi, F., Giszter, S., & Bizzi, E. (1993). Convergent force fields organized in the frog's spinal cord. *The Journal of neuroscience*, *13*(2), 467-491.

O'Leary, D. (1992). Development of connectional diversity and specificity in the mammalian brain by the pruning of collateral projections. *Curr Opinion Neurobiol*, *2*, 70-77.

Panerai, F., & Sandini, G. (1998). Oculo-motor stabilization reflexes: integration of inertial and visual information. *Neural Networks*, *11*(7), 1191-1204.

Papanikolopoulos, N. P., & Khosla, P. K. (1993). Adaptive robotic visual tracking: Theory and experiments. *IEEE Trans. on Automatic Control*, *38, N. 3*, 429–445.

Piaget, J., & Inhelder, B. (1969). *The psychology of the child.* New York: Basic Books.

Rack, P., & Westbury, D. (1969). The effects of lenght and stimulus rate on tension in the isometric cat soleus muscle. *Journal of Physiology*, *204*, 443-460.

Samson, C., Borgue, M. L., & Espiau, B. (1991). *Robot control: the task function approach.* Clarendon press, Oxford.

Sandini, G. (1997). Artificial systems and neuroscience. In M. Srinivasan (Ed.), *Proc. of the otto and martha fischbeck seminare on active vision.* ((abstract))

Sandini, G., Gandolfo, F., Grosso, E., & Tistarelli, M. (1993). Vision during action. In Y. Aloimonos (Ed.), *Active perception* (pp. 151–190). Lawrennce Erlbaum Associates.

Sandini, G., & Tagliasco, V. (1980). An anthropomorphic retina-like structure for scene analysis. *CGIP*, *14 No.3*, 365–372.

Sutton, R., & Barto, A. (1998). *Reinforcement learning: an introduction.* MIT

Press.
White, B., Castle, P., & Held, R. (1964). Observations on the development of visually guided reaching. *Child Development*, *35*, 349-364.
Yoshikawa, T. (1990). *Foundations of robotics, analysis and control.* MIT Press.